Rapid Communications

Coupled dipole oscillations of a mass-imbalanced Bose-Fermi superfluid mixture

Yu-Ping Wu, Xing-Can Yao, Xiang-Pei Liu, Xiao-Qiong Wang, Yu-Xuan Wang, Hao-Ze Chen, Youjin Deng, Yu-Ao Chen, and Jian-Wei Pan

Shanghai Branch, National Laboratory for Physical Sciences at Microscale and Department of Modern Physics, University of Science and Technology of China, Shanghai 201315, China;
CAS Center for Excellence and Synergetic Innovation Center in Quantum Information and Quantum Physics, University of Science and Technology of China, Hefei, Anhui 230026, China;
and CAS-Alibaba Quantum Computing Laboratory, Shanghai 201315, China

(Received 12 May 2017; published 22 January 2018)

Recent experimental realizations of superfluid mixtures of Bose and Fermi quantum gases provide a unique platform for exploring diverse superfluid phenomena. We study dipole oscillations of a double superfluid in a cigar-shaped optical dipole trap, consisting of ^{41}K and ^{6}Li atoms with a large mass imbalance, where the oscillations of the bosonic and fermionic components are coupled via the Bose-Fermi interaction. In our high-precision measurements, the frequencies of both components are observed to be shifted from the single-species ones, and exhibit unusual features. The frequency shifts of the ^{41}K component are upward (downward) in the radial (axial) direction, whereas the ^{6}Li component has downshifted frequencies in both directions. Most strikingly, as the interaction strength is varied, the frequency shifts display a resonantlike behavior in both directions, for both species, and around a similar location at the BCS side of the fermionic superfluid. These rich phenomena challenge the theoretical understanding of superfluids.

DOI: 10.1103/PhysRevB.97.020506

The past two decades have witnessed vast experimental progress in generating and manipulating ultracold quantum gases, which have emerged as a powerful tool for simulating many-body physics and particularly diverse superfluid and superconductivity phenomena [1–3]. Examples include weakly interacting Bose-Einstein condensates (BECs) [4,5], the topological Berezinskii-Kosterlitz-Thouless phase transition [6,7], emergent relativistic phenomena near the superfluid-to-Mott-insulator quantum critical point [8,9], and the crossover between a BEC and a BCS superfluid in fermionic systems [10,11]. Very recently, experimental realizations of Bose-Fermi double superfluids have been reported for ^{6}Li-^{7}Li, ^{6}Li-^{41}K, and ^{6}Li-^{174}Yb mixtures [12–14]. This is an important achievement, taking into account that, in the study of liquid helium, the strong interisotope interactions have prevented the long-sought goal of realizing simultaneous superfluidity in a ^{4}He-^{3}He mixture [15]. Many fascinating behaviors can emerge in this novel quantum matter owing to Bose-Fermi interactions, including topological p-wave Cooper pairing [16], Bose-Fermi dark solitons [17], and polaronic atom-trimer continuity [18]. Experimentally, although the measured critical velocity of a ^{6}Li-^{7}Li mixture can be mostly accounted for by a generalized Landau criterion, it has an unexplained strong reduction on the BEC side [19]. For a ^{6}Li-^{41}K double superfluid, quantized vortices, a hallmark of superfluidity, are simultaneously generated in both species, and several unconventional interaction-induced properties are observed [13].

The investigation of collective excitations is well known to be an important method for gaining insights into the physical properties of trapped BECs and strongly interacting Fermi gases [20–24]. The simplest collective dynamics is the dipole oscillation for the center-of-mass motion of all atoms. Therefore, characterizing the dipole oscillation would be the first step to understand interaction-induced effects in Bose-Fermi superfluid mixtures. If all of the bosonic and fermionic atoms have the same mass and experience the same trapping frequency, the dipole oscillation frequency is exactly given by the noninteracting result, i.e., the intra- and intercomponent interactions play no role in the dipole oscillation. This is known as the Kohn theorem [25,26]. In a ^{6}Li-^{7}Li superfluid mixture [12,19], the slightly different masses of the two isotopes break the dynamical symmetry, and the dipole oscillation of the bosonic ^{7}Li component has a downshifted frequency and a beating behavior in the oscillation amplitudes. These results are well explained by a phenomenological two-oscillator model with effective mean-field interactions [12]. Similar behaviors have been reported for a ^{6}Li-^{174}Yb superfluid mixture [14], in which the dynamical symmetry is heavily broken by the large mass imbalance.

In this Rapid Communication, we report on the study of the coupled collective dipole oscillations of a ^{6}Li-^{41}K superfluid mixture in a cigar-shaped optical dipole trap. We perform precise measurements of oscillations in both the axial and radial directions, and observe three features that have not been reported in the previous experiments [12,14,19]. First, both the bosonic and fermionic atoms have oscillation frequencies shifted from the single-species ones, although the frequency changes of the ^{6}Li component are small and only up to one and a half percent. Second, the frequency shifts of the ^{41}K component are opposite: downward (upward) in the axial (radial) direction, while the ^{6}Li component has downshifted frequencies in both directions. Most strikingly, as the system is tuned across the BEC-BCS crossover, the axial and radial frequency shifts both display a resonantlike behavior on the BCS side around

$1/k_F a_f = -0.2$, where k_F is the Fermi momentum and a_f is the scattering length of the ^{6}Li atoms. A phenomenological analysis, which takes into account the mean-field interactions and their effects on the density profiles of both species, can only qualitatively describe a small part of the experimental data.

Experimental procedure. The experimental procedure for preparing the Bose and Fermi superfluid mixture is similar to that of our previous works [13,27–29]. After the laser cooling and magnetic transport phase, the mixture of cold ^{6}Li and ^{41}K atoms is confined in an optically plugged magnetic trap in a dodecagonal glass cell with good optical access and an ultrahigh vacuum environment, where rf evaporation [30] of ^{41}K atoms is implemented and the ^{6}Li atoms are cooled sympathetically. Then, we load the cold Bose-Fermi mixture into a cigar-shaped optical dipole trap (wavelength 1064 nm, $1/e^2$ radius 35 μm) and apply two 3-ms Landau-Zener sweeps to prepare both species at their lowest hyperfine states. Next, the magnetic field B is ramped to 871 G, and a half-to-half spin mixture of the two lowest hyperfine states of ^{6}Li is prepared using successive rf sweeps. After 0.5 s forced evaporation, the clouds are adiabatically transferred into the final cigar-shaped optical trap (wavelength 1064 nm, $1/e^2$ radius 62.5 μm) with large trap volume. Further evaporation is accomplished by exponentially lowering the trap depth to 512 nK (^{41}K) and 1.00 μK (^{6}Li) in 3 s. Finally, the Bose and Fermi superfluid mixture is achieved with $N_B = 2.3 \times 10^5$ ^{41}K atoms of a condensate fraction $\geqslant 90\%$ and approximately $N_F = 1 \times 10^6$ ^{6}Li atoms at 0.06(1) Fermi temperature. The Thomas-Fermi radii of the ^{41}K component are about 4.4 μm radially and 86.3 μm axially, and the ^{6}Li component has a Fermi radii of about 25.3 μm radially and 363.8 μm axially. In the gravitation direction, the full overlap of the two species is achieved with a slightly off-centered distance of 10 μm at 871 G.

The oscillation experiment is performed within the plane perpendicular to the gravity direction. At the end of evaporation, the magnetic field is ramped in 200 ms to the value for the oscillation experiment, and is held for another 500 ms to achieve fully thermal equilibrium of the two species. The dipole oscillation in the axial direction is induced by adiabatically shifting the center position of the superfluid mixture to a distance of approximately 18.5 μm in the weakly confining direction z, and abruptly releasing the atom clouds in the trap. For the oscillation experiment in the radial direction, the optical trap depth is adiabatically ramped up to 1.90 μK (^{41}K) and 1.80 μK (^{6}Li) in 200 ms after the Bose and Fermi superfluid mixture is achieved. The radial dipole mode is excited by adiabatically displacing the optical trap center by approximately 5 μm in 20 ms with an acoustical optical modulator and quickly shifting it back to the initial position in 100 μs. The oscillation amplitudes are small enough to ensure the full overlapping of the two species during oscillation. After a variable holding time, the optical trap potential is suddenly switched off, and the atom clouds are expanded for 2 ms in the residual magnetic curvature. A specially designed imaging setup in the gravity direction is employed to simultaneously probe the two species [13], and the centers of the atom clouds are simultaneously recorded. With a high numerical aperture objective, an imaging resolution of 2.2 μm (2.5 μm) at 671 nm (767 nm) is obtained.

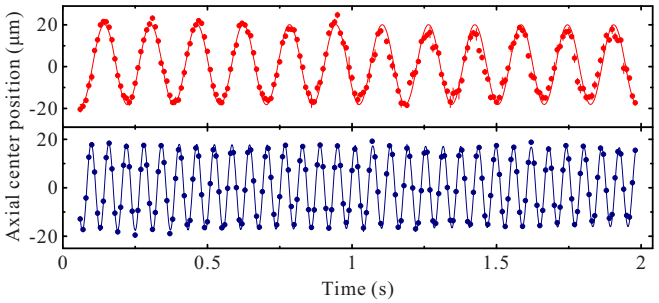

FIG. 1. Axial dipole oscillations of the ^{6}Li-^{41}K superfluid mixture at $B = 834$ G. Symbols are the center-of-mass positions of ^{41}K (top) and ^{6}Li (bottom) clouds, respectively. Solid lines are the fitting curves according to an exponentially damped sinusoid model.

The frequency shifts induced by the Bose-Fermi interaction are relatively small in magnitude, and this requests a highly stable and controllable system. In our experiment, with active stabilization methods, the magnetic field can be engineered with a high precision with ± 10 mG at $B = 834$ G, as calibrated by a rf spectroscopy of ^{41}K atoms. The laser intensity is controlled by a two-stage intensity stabilizing system, which leads to a long-term stability of 0.1%.

Experimental result. As an illustration, we consider the $B = 834$ G case, which is very close to the most precise location of the Feshbach resonance [31] and well satisfies the unitarity criterion. The recorded centers of the atom clouds after 2 ms of expansion are shown in Figs. 1 and 2, where each data point is averaged from at least four measurements that are postselected with atom number variation of both species less than 5%. The curves can be nicely approximated by single-frequency harmonic oscillations, and the damping rates are small, especially in the axial direction, where the oscillations of both species persist for more than 2 s without visible damping.

The experimental data are fitted by exponentially damped sinusoidal models. For the axial oscillations, the fits yield frequencies $\widetilde{\omega}_f^z = 2\pi \times 16.420(5)$ Hz for the fermionic ^{6}Li component and $\widetilde{\omega}_b^z = 2\pi \times 6.202(7)$ Hz for the bosonic ^{41}K atom cloud, with the error margins corresponding to one standard statistical deviation. The damping constants $\widetilde{\omega}_i^z \tau_i^z$ ($i = $ b,f) are larger than 10^3 for both species. In the radial direction, the frequencies are $\widetilde{\omega}_f^r = 2\pi \times 291.1(4)$ Hz (^{6}Li) and $\widetilde{\omega}_b^r = 2\pi \times 174.3(4)$ Hz (^{41}K), and the damping constants

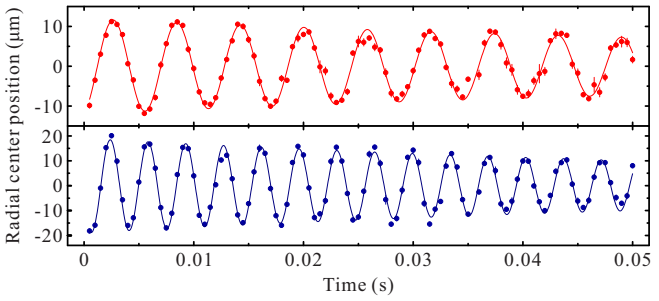

FIG. 2. Radial dipole oscillations of the ^{6}Li-^{41}K superfluid mixture at $B = 834$ G. Symbols are the center-of-mass positions of ^{41}K (top) and ^{6}Li (bottom) clouds, respectively. Solid lines are the fitting curves according to an exponentially damped sinusoid model.

are $\widetilde{\omega}_{\rm f}^r\tau_{\rm f}^r \simeq 142$ and $\widetilde{\omega}_{\rm b}^r\tau_{\rm b}^r \simeq 110$, respectively. The results are shown as the solid lines in Figs. 1 and 2, where nearly all of the data points lie on top of the fitting curves or have small deviations. This reflects the reliability of the fitting results and of the quoted error bars.

Comparison studies of the dipole oscillations are carried out for the single-species superfluids, consisting only of ^{6}Li or ^{41}K atoms. We obtain oscillation frequencies $\omega_{\rm f}^z = 2\pi \times 16.453(2)$ Hz (^{6}Li) and $\omega_{\rm b}^z = 2\pi \times 6.295(8)$ Hz (^{41}K) in the axial direction, and $\omega_{\rm f}^r = 2\pi \times 295.4(3)$ Hz (^{6}Li) and $\omega_{\rm b}^r = 2\pi \times 170.7(5)$ Hz (^{41}K) in the radial direction. The relative frequency shift is then computed as $\Delta\omega/\omega \equiv (\omega - \widetilde{\omega})/\omega$, with positive (negative) values for downward (upward) shifts. We obtain $\Delta\omega_{\rm b}^z/\omega_{\rm b}^z = +1.5(2)\%$ (^{41}K) and $\Delta\omega_{\rm f}^z/\omega_{\rm f}^z = +0.20(3)\%$ (^{6}Li) for the axial oscillations, and $\Delta\omega_{\rm b}^r/\omega_{\rm b}^r = -2.1(4)\%$ and $\Delta\omega_{\rm f}^r/\omega_{\rm f}^r = +1.5(2)\%$ for the radial oscillations.

A careful analysis suggests that the uncertainty of the axial trap frequencies induced by the highly controllable magnetic field is negligibly small, and that the long-term drifts of the radial frequencies introduced by the laser intensity would be around 0.05%, much smaller than the statistical errors. Moreover, since we are interested in the frequency difference, such long-term drifts are suppressed by alternative measurements for the single- and two-species superfluids. Further, by adjusting loading parameters, we also make sure that the temperature and atom numbers of ^{6}Li and ^{41}K are approximately identical in the two cases. Thus, frequency shift induced by atom numbers and temperature is greatly suppressed.

By applying the same procedures for the experiment and data analyses, we study the coupled dipole oscillations across the BEC-BCS crossover in the range of [767 G, 862 G] for the magnetic field. The damping rates are small in the entire parameter regime: the damping constants are bigger than 10^3 in the axial direction and are between 100 and 200 for the radial oscillations. The results for the frequency shifts are shown in Figs. 3 and 4. They display a few interesting features that have not been reported in the previous experiments [12,14,19].

First, it is confirmed that the Bose-Fermi interaction can lead to frequency changes in both the bosonic and fermionic superfluid components. Note that, since the cloud size of the bosonic atoms is smaller than that of the fermionic atoms, it is more difficult to induce a frequency shift in the latter. Indeed, no frequency change was observed in the dipole oscillations of the fermionic ^{6}Li cloud in ^{6}Li-^{7}Li [12,19]. In our case, the ^{6}Li atom cloud has a smaller frequency shift than the ^{41}K component (Figs. 3 and 4). Nevertheless, the existence of frequency shifts is well supported by the fact that the experimental data are far beyond the statistical uncertainties. We attribute the frequency shifts in the fermionic component to the large mass imbalance of the ^{41}K and ^{6}Li atoms, which can lead to pronounced interaction effects. For instance, it is observed that the repelling from the ^{41}K superfluid can induce a density-profile depression in the center of the ^{6}Li component [13].

Second, the dipole oscillation of the bosonic ^{41}K component has an upshifted frequency in the radial direction and a downshifted one in the axial direction. As shown in

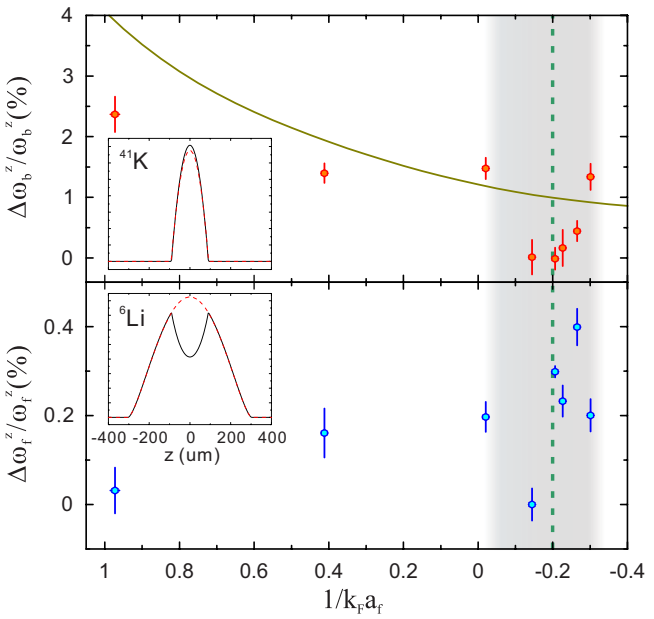

FIG. 3. Frequency shifts of axial dipole oscillations of the ^{6}Li-^{41}K superfluid mixture in the BEC-BCS crossover. Circles are measured frequency shifts of ^{41}K (top, red) and ^{6}Li (bottom, blue) atoms. The solid line is the theoretical predicted ^{41}K frequency shift from a phenomenological model that takes into account the interaction-induced alternations of density distributions. The green dashed line marks the position of $1/k_Fa_f = -0.2$ and the gray shadow shows the resonantlike region. Error bars represent one standard deviation. Insets are the numerically calculated density profiles of the ^{41}K (top) and ^{6}Li (bottom) cloud at 834 G, where the black solid lines are for superfluid mixture and the red dashed lines are for single-species superfluids.

Ref. [12], the frequency downshift can be straightforwardly explained using a phenomenological model with mean-field interactions. However, it is not clear what leads to the frequency upshifts. A possible explanation is scattering between normal components in the superfluid mixture; such a dissipation-induced coupling might drive the two species to oscillate with intermediate frequencies. The radial dipole oscillations have a frequency that is higher than the axial one by about 20 times, and are expected to suffer from more severe thermal effects.

Third, as the interaction strength is varied, a resonantlike behavior emerges in both the axial and radial oscillations, for both the Bose and Fermi species, and at a similar location of approximately $1/k_Fa_f = -0.2$ (BCS side) within a window of a size about 0.2. The radial and axial frequency shifts of the ^{41}K component exhibit a pronounced dip near $1/k_Fa_f = -0.2$, where the axial downshift drops to nearly zero and the radial upshift reaches a maximal value of about 4.5%. The frequency shifts of the fermionic ^{6}Li superfluid also display a nonsmooth behavior around $1/k_Fa_f = -0.2$. We mention that the damping rates remain approximately constant in the BEC-BCS crossover for both the axial and radial oscillations.

Phenomenological analysis. It is challenging to provide a first-principles calculation for the dipole oscillations of Bose-Fermi superfluid mixtures. In the previous works [12,14,19],

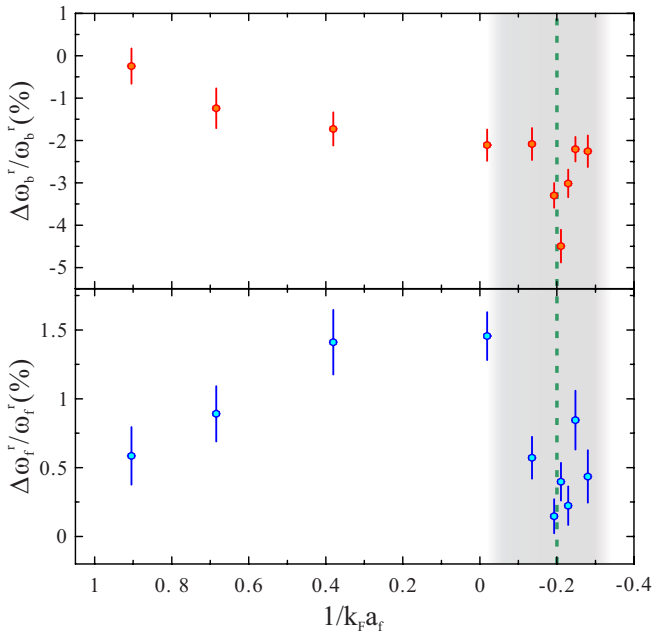

FIG. 4. Frequency shifts of radial dipole oscillations of the ^{6}Li-^{41}K superfluid mixture in the BEC-BCS crossover. Circles are measured frequency shifts of ^{41}K (top, red) and ^{6}Li (bottom, blue) atoms. The green dashed line marks the position of $1/k_Fa_f = -0.2$ and the gray shadow shows the resonantlike region. Error bars represent one standard deviation.

to explain the frequency downshifts, the bosonic component is considered as a pointlike impurity immersed in a Fermi superfluid, and the effective potential seen by the bosons is the sum of the trapping potential and the repulsive mean-field Bose-Fermi interaction, calculated within the local density approximation. To further account for the beating behavior in the oscillation amplitude, a model of two oscillators coupled by the mean-field interspecies interaction is introduced [12].

However, the Bose-Fermi interactions in the ^{6}Li-^{41}K superfluid mixture are very pronounced and can lead to a significant depression of the density distribution of the ^{6}Li cloud [13], which is ignored in the above pointlike treatment. On the basis of the coupled hydrodynamic description, the density distribution of the superfluid mixture in the overlapping region can be expressed as [32,33]

$$\begin{aligned} n_b(\mathbf{r}) &= (1/g_b)[\mu_b - V_b(\mathbf{r}) - 2g_{bf}n_f(\mathbf{r})], \\ n_f(\mathbf{r}) &= n_f^0\{(1/g_b\mu_f^0)[g_b\mu_f - g_{bf}\mu_b - g_bV_f(\mathbf{r}) \\ &\quad + g_{bf}V_b(\mathbf{r}) + 2g_{bf}^2n_f(\mathbf{r})]\}^{1/\gamma}. \end{aligned} \quad (1)$$

n_b and n_f are the superfluid densities for the bosonic and fermionic components, respectively; by definition, n_f also represents the density of ^{6}Li atoms in a single spin state. Symbols n_f^0 and μ_f^0 are the reference particle number density and the chemical potential of the ^{6}Li atoms, respectively, $g_{bf} = 2\pi\hbar^2a_{bf}/m_{bf}$ and $g_b = 4\pi\hbar^2a_b/m_b$ are the Bose-Fermi and the Bose-Bose interaction coupling constants, respectively, and $m_{bf} = m_bm_f/(m_b + m_f)$ is the ^{6}Li-^{41}K reduced mass. The scattering lengths are $a_{bf} = 60.2a_0$ and $a_b = 60.5a_0$ (a_0 is the Bohr radius) [13]. Symbol γ is the polytropic index of the equation of state of the strongly interacting Fermi gas [34–36]. For $B = 834$ G, the calculated static density distributions are shown in the insets of Fig. 3, clearly displaying a density depression in the ^{6}Li atom cloud.

The depression of the ^{6}Li density, if it were treated statically, might introduce an effective attractive potential for the ^{41}K cloud. However, since the maximum relative velocity is far below the critical velocity, e.g., $v_{max}^z \simeq 2.5$ mm/s $\ll v_{c,f}^z \simeq 17$ mm/s at the unitary limit [19,37], the depression in the ^{6}Li density should adiabatically follow the movement of the ^{41}K cloud. The effective potential seen by the ^{41}K atoms is then expressed as

$$\widetilde{V}_b(\mathbf{r}_1) = \frac{\int[V_b(\mathbf{r}+\mathbf{r}_1) + 2g_{bf}n_f(\mathbf{r},\mathbf{r}_1)] \times n_b(\mathbf{r})d\mathbf{r}}{\int n_b(\mathbf{r})d\mathbf{r}}, \quad (2)$$

where $\mathbf{r}_1$ is the center-of-mass position of the ^{41}K BEC, and $n_f(\mathbf{r},\mathbf{r}_1)$ is the $\mathbf{r}_1$-dependent density distribution of the ^{6}Li superfluid, which varies with the movement of the ^{41}K cloud. The potential in Eq. (2) is numerically calculated for the whole range of the BEC-BCS crossover and the oscillation frequency of the ^{41}K component is given by $\widetilde{\omega}_b^z = \sqrt{(\frac{\partial^2\widetilde{V}_b(\mathbf{r}_1)}{\partial z^2}|_{\mathbf{r}_1=0})/m_b}$. The resulting frequency downshifts, shown as the solid line in Fig. 3, exhibit similar trends and decrease from the BEC to BCS sides of the crossover. The deviations on the BEC side might be caused by the deformation of the ^{41}K density profile during oscillations, where the ^{6}Li density is significantly enhanced compared to the BCS regime.

In conclusion, despite that the frequency shifts are relatively small, the highly stable and controllable system enables us to obtain high-precision experimental data of big signal-to-noise ratio. They demonstrate that the coupled dipole oscillations of the ^{6}Li-^{41}K superfluid mixture, the simplest collective mode, show a variety of rich behaviors, particularly the pronounced dependence on the interacting strength. The behaviors can only be partly described within the current theoretical treatments and challenge theorists to further improve the models. The resonantlike frequency changes occur both for the axial and radial directions and on a similar location in the regime of a strongly attractive Fermi gas with $1/k_Fa_f = -0.2$. An immediate question arises then: does this imply some unknown universal mechanism? There are thus far only three successful realizations of Bose-Fermi superfluid mixtures, and our experimental results of the coupled dipole oscillations offer a promising prospect that due to Bose-Fermi interaction, such double-superfluid mixtures could exhibit rich static and dynamic quantum phenomena, novel quantum phases, and phase transitions.

Acknowledgments. We are indebted to C. Salomon and H. Zhai for valuable discussions. This work has been supported by the NSFC of China, the CAS, and the National Fundamental Research Program (under Grants No. 2013CB922001 and No. 2016YFA0301600). Y.-P. Wu, X.-C. Yao, and X.-P. Liu contributed equally to this work.

[1] W. Ketterle, Rev. Mod. Phys. **74**, 1131 (2002).

[2] I. Bloch, J. Dalibard, and W. Zwerger, Rev. Mod. Phys. **80**, 885 (2008).

[3] I. Bloch, J. Dalibard, and S. Nascimbene, Nat. Phys. **8**, 267 (2012).

[4] M. H. Anderson, J. R. Ensher, M. R. Matthews, C. E. Wieman, and E. A. Cornell, Science **269**, 198 (1995).

[5] K. B. Davis, M. O. Mewes, M. R. Andrews, N. J. van Druten, D. S. Durfee, D. M. Kurn, and W. Ketterle, Phys. Rev. Lett. **75**, 3969 (1995).

[6] F. S. Cataliotti, S. Burger, C. Fort, P. Maddaloni, F. Minardi, A. Trombettoni, A. Smerzi, and M. Inguscio, Science **293**, 843 (2001).

[7] Z. Hadzibabic, P. Kruger, M. Cheneau, B. Battelier, and J. Dalibard, Nature (London) **441**, 1118 (2006).

[8] M. Endres, T. Fukuhara, D. Pekker, M. Cheneau, P. Schauß, C. Gross, E. Demler, S. Kuhr, and I. Bloch, Nature (London) **487**, 454 (2012).

[9] D. Greif, M. F. Parsons, A. Mazurenko, C. S. Chiu, S. Blatt, F. Huber, G. Ji, and M. Greiner, Science **351**, 953 (2016).

[10] C. A. Regal, M. Greiner, and D. S. Jin, Phys. Rev. Lett. **92**, 040403 (2004).

[11] M. W. Zwierlein, C. A. Stan, C. H. Schunck, S. M. F. Raupach, A. J. Kerman, and W. Ketterle, Phys. Rev. Lett. **92**, 120403 (2004).

[12] I. Ferrier-Barbut, M. Delehaye, S. Laurent, A. T. Grier, M. Pierce, B. S. Rem, F. Chevy, and C. Salomon, Science **345**, 1035 (2014).

[13] X.-C. Yao, H.-Z. Chen, Y.-P. Wu, X.-P. Liu, X.-Q. Wang, X. Jiang, Y. Deng, Y.-A. Chen, and J.-W. Pan, Phys. Rev. Lett. **117**, 145301 (2016).

[14] R. Roy, A. Green, R. Bowler, and S. Gupta, Phys. Rev. Lett. **118**, 055301 (2017).

[15] J. Tuoriniemi, J. Martikainen, E. Pentti, A. Sebedash, S. Boldarev, and G. Pickett, J. Low Temp. Phys. **129**, 531 (2002).

[16] J. Rysti, J. Tuoriniemi, and A. Salmela, Phys. Rev. B **85**, 134529 (2012).

[17] M. Tylutki, A. Recati, F. Dalfovo, and S. Stringari, New J. Phys. **18**, 053014 (2016).

[18] Y. Nishida, Phys. Rev. Lett. **114**, 115302 (2015).

[19] M. Delehaye, S. Laurent, I. Ferrier-Barbut, S. Jin, F. Chevy, and C. Salomon, Phys. Rev. Lett. **115**, 265303 (2015).

[20] S. Stringari, Phys. Rev. Lett. **77**, 2360 (1996).

[21] D. S. Jin, J. R. Ensher, M. R. Matthews, C. E. Wieman, and E. A. Cornell, Phys. Rev. Lett. **77**, 420 (1996).

[22] M. Bartenstein, A. Altmeyer, S. Riedl, S. Jochim, C. Chin, J. H. Denschlag, and R. Grimm, Phys. Rev. Lett. **92**, 203201 (2004).

[23] A. Altmeyer, S. Riedl, C. Kohstall, M. J. Wright, R. Geursen, M. Bartenstein, C. Chin, J. H. Denschlag, and R. Grimm, Phys. Rev. Lett. **98**, 040401 (2007).

[24] J.-Y. Zhang, S.-C. Ji, Z. Chen, L. Zhang, Z.-D. Du, B. Yan, G.-S. Pan, B. Zhao, Y.-J. Deng, H. Zhai, S. Chen, and J.-W. Pan, Phys. Rev. Lett. **109**, 115301 (2012).

[25] W. Kohn, Phys. Rev. **123**, 1242 (1961).

[26] F. Dalfovo, S. Giorgini, L. P. Pitaevskii, and S. Stringari, Rev. Mod. Phys **71**, 463 (1999).

[27] Y.-P. Wu, X.-C. Yao, H.-Z. Chen, X.-P. Liu, X.-Q. Wang, Y.-A. Chen, and J.-W. Pan, J. Phys. B **50**, 094001 (2017).

[28] H.-Z. Chen, X.-C. Yao, Y.-P. Wu, X.-P. Liu, X.-Q. Wang, Y.-X. Wang, Y.-A. Chen, and J.-W. Pan, Phys. Rev. A **94**, 033408 (2016).

[29] H.-Z. Chen, X.-C. Yao, Y.-P. Wu, X.-P. Liu, X.-Q. Wang, Y.-A. Chen, and J.-W. Pan, Appl. Phys. B **122**, 281 (2016).

[30] W. Ketterle and N. J. van Druten, Adv. Atomic, Molecular, and Optical Phys. **37**, 181 (1996).

[31] G. Zürn, T. Lompe, A. N. Wenz, S. Jochim, P. S. Julienne, and J. M. Hutson, Phys. Rev. Lett. **110**, 135301 (2013).

[32] T. Ozawa, A. Recati, M. Delehaye, F. Chevy, and S. Stringari, Phys. Rev. A **90**, 043608 (2014).

[33] W. Wen, B. Chen, and X. W. Zhang, J. Phys. B **50**, 035301 (2017).

[34] C. Menotti, P. Pedri, and S. Stringari, Phys. Rev. Lett. **89**, 250402 (2002).

[35] N. Navon, S. Nascimbène, F. Chevy, and C. Salomon, Science **328**, 729 (2010).

[36] Y.-P. Wu, X.-C. Yao, X.-P. Liu, X.-Q. Wang, Y.-X. Wang, H.-Z. Chen, M. Maraj, Y. Deng, Y.-A. Chen, and J.-W. Pan, arXiv:1702.08326.

[37] W. Weimer, K. Morgener, V. P. Singh, J. Siegl, K. Hueck, N. Luick, L. Mathey, and H. Moritz, Phys. Rev. Lett. **114**, 095301 (2015).